

Exploring Percolative Landscapes: Infinite Cascades of Geometric Phase Transitions

P. N. Timonin¹, Gennady Y. Chitov²

*(1) Physics Research Institute, Southern Federal University,
344090, Stachki 194, Rostov-on-Don, Russia, pntim@live.ru*

*(2) Department of Physics, Laurentian University
Sudbury, Ontario P3E 2C6, Canada, gchitov@laurentian.ca*

The evolution of many kinetic processes in 1+1 (space-time) dimensions results in 2d directed percolative landscapes. The active phases of these models possess numerous hidden geometric orders characterized by various types of large-scale and/or coarse-grained percolative backbones that we define. For the patterns originated in the classical directed percolation (DP) and contact process (CP) we show from the Monte-Carlo simulation data that these percolative backbones emerge at specific critical points as a result of continuous phase transitions. These geometric transitions belong to the DP universality class and their nonlocal order parameters are the capacities of corresponding backbones. The multitude of conceivable percolative backbones implies the existence of infinite cascades of such geometric transitions in the kinetic processes considered. We present simple arguments to support the conjecture that such cascades of transitions is a generic feature of percolation as well as many others transitions with nonlocal order parameters.

Keywords: kinetic processes, phase transitions, percolation.

PACS numbers: 64.60.Cn, 05.70.Jk, 64.60.Fr

1. Introduction

The cornerstones of modern civilization are various types of networks: telecommunications, electric power supply, Internet, warehouse logistics, to name a few. Their proper functioning is of great importance and many studies have been devoted to their robustness against various kinds of damages [1, 2]. Yet there are other aspects of the network quality – their abilities for restoration, repairing, renovation and upgrades. To assess these abilities, we should know the details of the network structure which are responsible for these features. Also these details should be implemented in the constructions of new networks. Thus, the useful feature of a network can be the existence in it some subset (“percolative backbone”) spreading through the whole network, which can be used for the future upgrades or restoration. For example, the transportation or communication networks can be modernized by placing more powerful transmitters on the backbone’s nodes and discarding obsolete ones on the rest of the nodes. As well, in the process of damaged network restoration, one can link the remanent backbone’s nodes to quickly restore the supply on a large territory.

Another conceivable way of network renovation is to merge the groups of several nearby nodes into a single hub. The hubs’ network may comprise the backbone of the whole network to

make such ‘coarse-grained’ upgrade most effective. Percolative properties of clustered and coarse-grained networks have been intensively studied in recent literature. [2–5]

However, the majority of the existing networks appeared as a result of some stochastic process spreading in some region according to its landscape, population, resources distribution, etc. Are they renewable or reparable in the senses described above is not known. Yet it can be established for the model kinetic processes via simple numerical Monte Carlo (MC) simulations. Here we use MC technique to explore $2d$ (space-time) percolation patterns (networks) emerging in directed percolation (DP), contact process (CP) [6, 7] and replication process of Ref. [8]. We show that under variations of control parameters the percolation patterns of these processes undergo a series of geometrical phase transitions in which they acquire various percolative backbones. We also present arguments that such cascades are a generic feature of percolation as well as many other transitions governed by the nonlocal order parameters

2. Directed percolation

The directed percolation on $2d$ (space-time) lattice shown in Fig. 1 can be considered as kinetic process. Setting the steps in the temporal or spatial directions equal to unity, the spacing of the DP lattice in Fig. 1 is $a = \sqrt{2}$. Each site can be in one of two states - wet or dry (filled-empty, infected- healthy etc., in other contexts). In the DP variant called “bond DP” (BDP) at each time step the percolative bonds are placed randomly with probability p between nearest neighbor sites in the columns t and $t+1$. If such bond connects a wet site at column t with its neighbor at column $t+1$ then the last also becomes wet, otherwise it stays dry. There can be two outcomes of this time evolution starting from some initial configuration of wet sites at $t = 0$ – either the wet sites become extinct or they persist for infinite times. The first scenario takes place for $p < p_{BDP} \approx 0.6447$ and it corresponds to the absorbing phase, while the infinite proliferation of wet sites appears for $p > p_{BDP}$ resulting in the active or percolating phase. [6, 7]

The main tool for the studies of the DP-type kinetic processes is the Monte-Carlo simulations. They numerically mimic stochastic evolution based on the model's transfer probabilities defined as the probability of possible configurations at time $t+1$ given the configuration at time t . We denote it as $P(n_{i,t+1} | n_{i-1,t}, n_{i+1,t})$. Here all sites are endowed with occupation numbers (a.k.a. lattice gas parameters) $n_{i,t} = 0, 1$; where 1 corresponds to wet (filled) sites and 0 is ascribed to dry (empty) ones. For the BDP the transfer probabilities are $P(1|0,1) = P(1|1,0) = p$, $P(1|1,1) = p(2-p)$, $P(1|0,0) = 0$; $P(0|a,b) = 1 - P(1|a,b)$.

Note that the probability of site to become wet when it has two wet ancestors is the probability to have at least one bond attached to the site, i. e. $1 - (1-p)^2 = p(2-p)$. In this work we implement the Monte-Carlo simulations with parallel update, in which the configurations of all sites are updated simultaneously in one time step. This very simple numerical procedure results in raw data whence various (BDP) percolating patterns (networks of wet sites with $n_{i,t} = 1$) can be revealed. For every trial with $p > p_{BDP}$ we get chaotically looking percolative patterns which appear to have

only two features in common: wet sites always spread to infinite time and the number of wet sites at large times is approximately the same at all trials for a given value of p . In other respects these patterns are seemingly disordered and devoid any structure for all $p > p_{BDP}$. However, we prove below that this impression is deceptive. Actually, the percolation patterns in this model are not utterly chaotic but possess many types of intrinsic geometrical structures that change many times with variation of p .

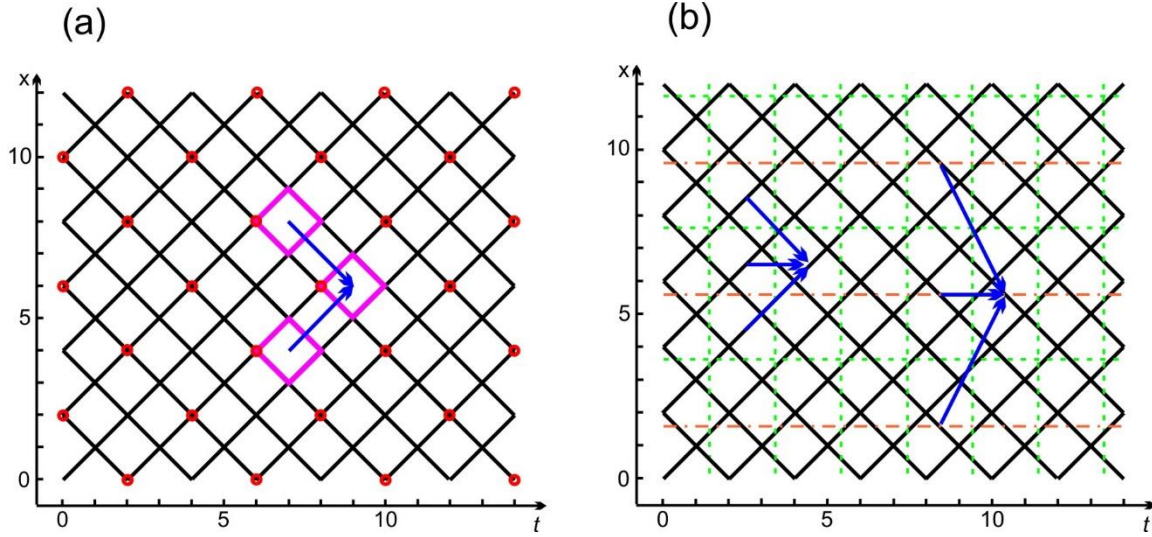


Fig.1. *Examples of coarse-grained lattices (backbones) for the BDP process.* The original tilted square lattice for the BDP process with spacing $a = \sqrt{2}$ is shown by solid lines on both panels. (a) The tilted square sublattice with the spacing $2a$ and the sites denoted by red circles. Those circles also indicate the leftmost nodes of plaquettes (magenta squares) discussed in the text. (b) Division of the original lattice into 4-site cells (dashed lines) and into 2-site cells (dashed and dot-dashed lines). Colored arrows show the bonds for percolation on resulting coarse-grained lattices.

To corroborate the above statements let us first check whether the conventional percolative phase on the original tilted square BDP lattice with spacing a (cf. Fig. 1) also contains a percolative cluster of the wet sites on the sublattice with spacing $2a$ shown in Fig. 1(a) with red circles. We consider sets of the sublattice sites belonging to the original pattern of directed percolation to determine whether there are paths connecting the nearest neighbors in this set, such that these paths traverse the whole sample in time direction thus forming the sublattice backbone of this particular percolation pattern. For such paths one can easily calculate the number of sites in the backbone at arbitrary t via a recursive numerical procedure. First we need to find connected backbone sites (CBS) at $t = 2$, i. e., those having nearest neighbors from the set at $t = 0$, then we search for CBS at $t = 4$ having nearest neighbors in CBS at $t = 2$, and so on. In doing so over many trials we can obtain at every even time step t the average number $N_{CBS}(t)$ of sites in the backbone connected by the nearest-neighbor paths to $t = 0$.

Analytical representation of $N_{CBS}(t)$ is readily given as an average of the order parameter operator

$$2N_{CBS}(t)/N = \langle \mathcal{P}_{i,t} \rangle \equiv P(t), \quad \mathcal{P}_{i,t} = \sum_{\sigma} O_{i,t}(\sigma) \quad (1)$$

$$O_{i,t}(\sigma) = n_{2i,2t} \prod_{\tau=1}^{t-1} n_{2\left(i + \sum_{k=\tau}^{t-1} \sigma_k\right), 2\tau} \quad (2)$$

Here all auxiliary parameters σ can admit two values $\sigma_k = \pm 1$ and the angular brackets denote the averaging with the distribution function

$$W_{BDP} = \prod_{i,t} P(n_{i,t+1} | n_{i-1,t}, n_{i+1,t}) \equiv e^{-H_{BDP}} / Z, \quad H_{BDP} = \sum_{i,t} H_{i,t}$$

$$H_{i,t} = n_{i,t+1} \left[\ln \frac{p}{2-p} n_{i+1,t} n_{i-1,t} + \ln \frac{1-p}{p} (n_{i+1,t} + n_{i-1,t}) + i\psi (1-n_{i+1,t})(1-n_{i-1,t}) \right] - 2 \ln(1-p) n_{i,t} \quad (3)$$

Here the auxiliary variable of integration ψ is introduced to enforce the model rule $(0,0) \rightarrow 0$. For more details on this formalism, see [8].

W_{BDP} gives the probability of every configuration in BDP process for given initial values of $n_{i,0}$. Each set of σ defines the nearest-neighbors path on the sublattice connecting the site with coordinates $(2i, 2t)$ to some sublattice site at $t = 0$. Operator $O_{i,t}(\sigma)$ is equal to 1 if the path belong to the percolation cluster of BDP process and zero otherwise. Thus its average in Eq. (1) is the probability that site $(2i, 2t)$ belongs to the sublattice backbone. For cyclic boundary conditions in space direction the order parameter $P(t)$ in Eq. (1) does not depend on the site index $2i$.

It follows from Eq. (2)

$$O_{i,t+1}(\sigma) = n_{2i,2t+2} \left(O_{i-1,t}(\sigma') \delta_{\sigma_t, -1} + O_{i+1,t}(\sigma') \delta_{\sigma_t, 1} \right) \quad (4)$$

where σ' is σ without σ_t . Summing this equation over σ we get

$$\mathcal{P}_{i,t+1} = n_{2i,2t+2} (\mathcal{P}_{i-1,t} + \mathcal{P}_{i+1,t}). \quad (5)$$

Thus for any given configuration of $n_{i,t}$, operator $\mathcal{P}_{i,t}$ can be calculated iteratively starting from $\mathcal{P}_{i,0} = n_{2i,0}$. Just this procedure is implemented in our MC calculations while the average $\langle \mathcal{P}_{i,t} \rangle = P(t)$ is obtained via the averaging over MC trials. The results are presented in Fig. 2. They show that $P(t)$ goes to zero at large t if $p < p_c \approx 0.6635$ while $P(\infty) \neq 0$ for $p > p_c$. This means that the stable BDP percolation patterns undergo phase transition at p_c in which they acquire the infinite 'sublattice backbone'. The scaling indexes $\alpha \approx 0.16$ and $\nu_{||} \approx 1.73$ that we found for this transition are those of the DP universality class.

Similar analysis can be carried out for other type of backbones. In particular, we can easily modify the previous procedure to deal with the backbone formed by a sublattice with spacing $4a$

and sites located at the points $(4i, 4t)$. We just need to substitute $2 \rightarrow 4$ in the subscripts entering equation (2) to obtain the string operator, and then, the order parameter (1) for such a sublattice. To treat the backbones obtained by coarse graining of the original lattice, (cf. 2-site and 4-site cells shown in Fig. 1(b)), we introduce the occupation number of the cells $v_{j,\tau} = 0,1$ as

$$v_{j,\tau} = \mathcal{G} \left(\sum_{i,t \in c_{j,\tau}} n_{i,t} - f \right), \quad (6)$$

where \mathcal{G} is the Heaviside step function defined such that $\mathcal{G}(x \geq 0) = 1$ and the summation runs over all sites in the cell $c_{j,\tau}$.

This new “renormalized” occupation number on the coarse-grained lattice depends on the overall cell filling f , and different choices of parameter f correspond to different types of backbones. We can as well choose different bonds for the cell percolation. For instance, as one can see from Fig. 1(b), we can allow percolation from three ancestors (nearest and next-nearest) or ban percolation from the nearest ancestor thus eliminating the horizontal bond. So we obtain different types of backbones. Note that in the case of percolation over a sublattice or via plaquettes, only two nearest ancestors are present on the renormalized lattice, cf. Fig. 1(a), so the above comments do not apply for the latter cases.

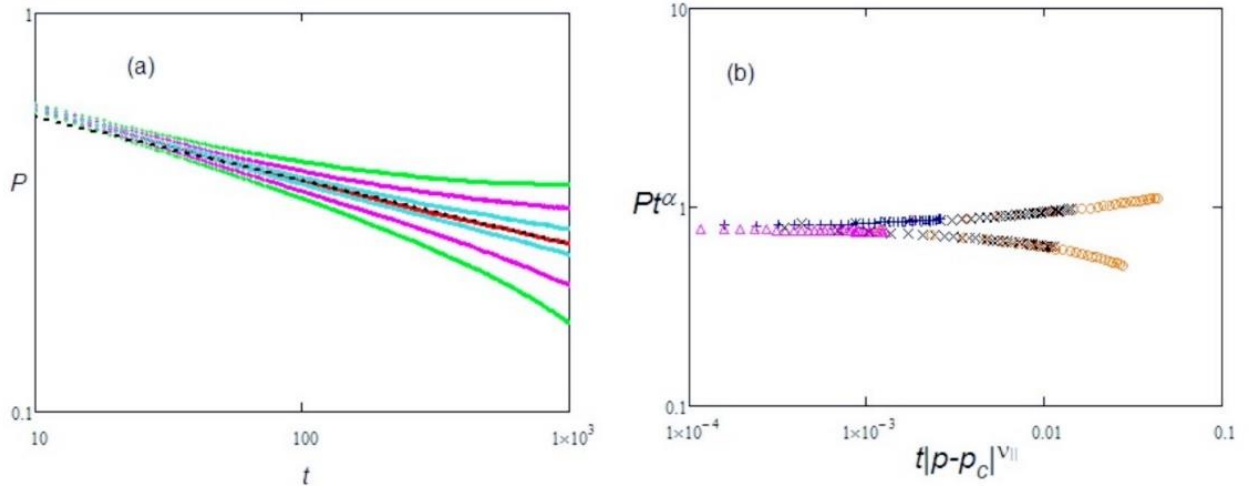



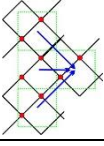
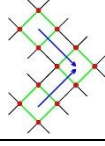

Fig. 2. *BDP on the 2a sublattice.* (a) MC simulations of relaxation of the BDP sublattice percolation capacity $P(t)$ for series of p near $p_c \approx 0.6635$, from top to bottom: $p=0.6665, 0.665, 0.664, 0.6635, 0.663, 0.662, 0.661$. The dashed line corresponds to the power law $0.8/t^\alpha$, with $\alpha = 0.16$. (b) Collapse of the curves from (a) onto a single scaling function. Fitting gives the values of $\nu_{||} \approx 1.731$ and $p_c = 0.6635$. The chain studied has 20000 sites with cyclic boundary conditions and raw data are averaged over 200 trials. Initial state is fully occupied one.

We ran simulations and scaling analyses explicitly for several backbones appearing in the percolative patterns for this model. The results are summarized in Table I. The appearance of a new percolative backbone at the specific critical value p_c constitutes a genuine second order phase transition with specific nonlocal order parameter (capacity of corresponding backbone) similar to

the one defined by equations (2), (3). The critical indices we obtained from the collapse of the appropriate scaling curves for the critical points presented in Table I indicate that all these geometric phase transitions belong to the DP universality class. Note that the plaquette, 2-site and 4-site hubs backbones with $f = 1$ and $h = 1$ always exist in the BDP patterns while backbones with the 2-site and 4-site hubs and $f = 1, h = 0$ appear simultaneously (within our precision) with the $f = 2$ plaquette percolative backbone at $p_c \approx 0.646$. For a more visual presentation of our results, several percolative patterns obtained by direct MC simulations along with corresponding schematic pictures of their backbones are shown in Fig. 3.

It should be obvious at this point, that one can construct in this way many other percolative backbones by varying sublattices, coarse-grained cells and/or percolative bonds. We conjecture that in the BDP model there is an infinite cascade of geometric phase transitions where various new percolative backbones emerge.

Table 1. Critical points of geometric phase transitions where different backbones appear. The parameter h designate the presence ($h = 1$) or absence ($h = 0$) of horizontal bonds in the percolative backbone.

Sublattices		2-site hubs			Plaquettes		4-site hubs		
									
Spacing	p_c	f	h	p_c	f		f	h	p_c
2a	0.663(5)	1	1	$p_{BDP}=0.6447$	1	$p_{BDP}=0.6447$	2	1	$p_{BDP}=0.6447$
4a	0.677(6)	1	0	0.646(7)	2	0.646(5)	2	0	0.646(4)
		2	1	0.656(2)	3	0.671(2)	3	1	0.657(4)
		2	0	0.696(3)	4	0.742(5)	3	0	0.682(7)
							4	1	0.710(2)
							4	0	0.759(5)

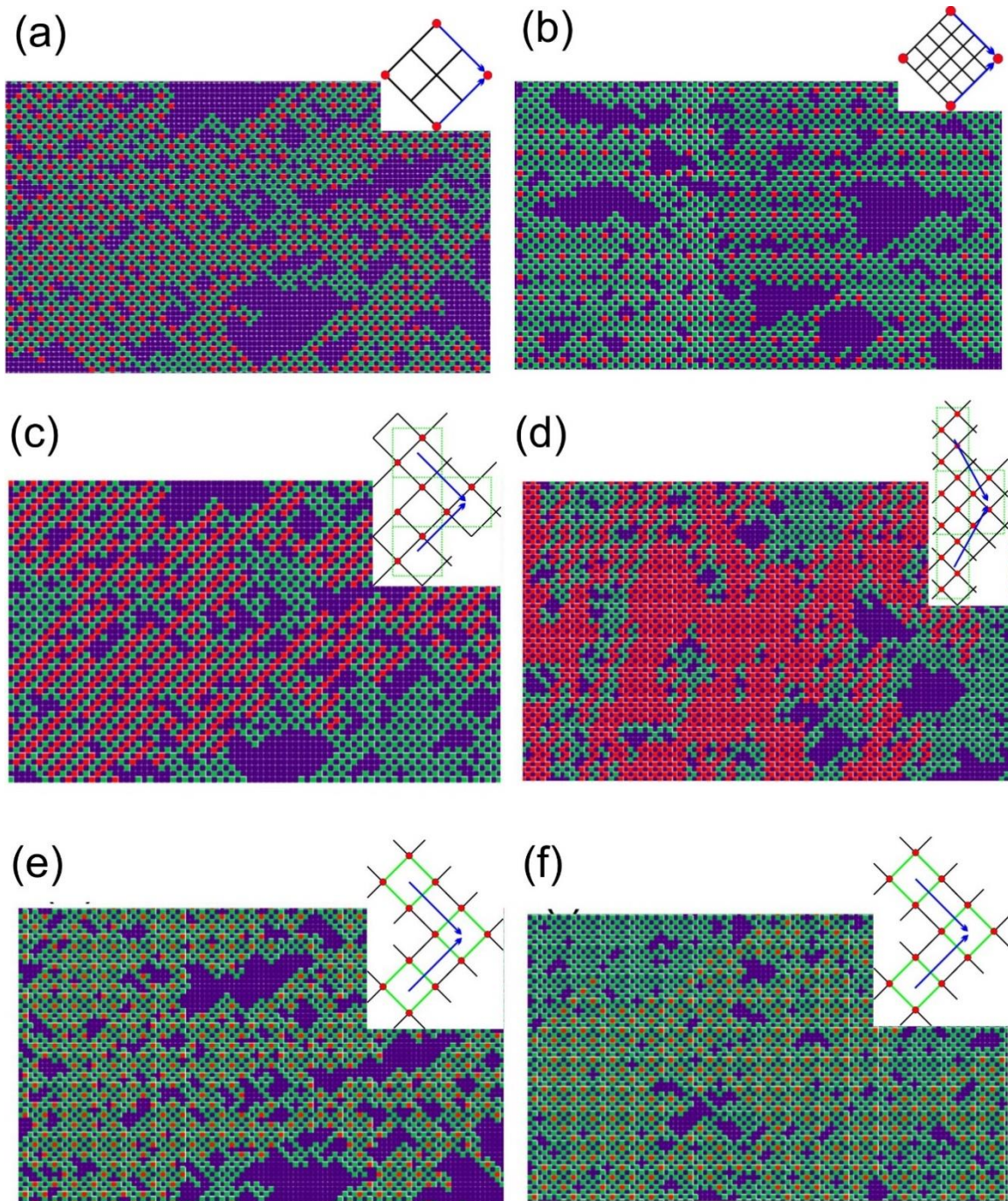


Fig. 3. *BDP patterns*. The fragments of steady patterns of BDP process (green squares) with backbones (red squares). (a) $p = 0.67$, $2a$ sublattice backbone, (b) $p = 0.68$, $4a$ sublattice backbone (c) $p = 0.68$, 2-site cells' backbone with next-nearest bonds, (d) $p = 0.76$, 4-site cells' backbone with next-nearest bonds, (e) $p = 0.68$, plaquettes' backbone, $f = 3$, red squares are centers of percolative plaquettes, (f) $p = 0.75$, plaquettes' backbone, $f = 4$.

3. Contact process

Now we address another popular and well-studied kinetic model, namely, the contact process (CP). This model is used, e.g. to describe spreading of plant infections or plant population via dissemination of seeds [6, 7]. The model has two parameters p and q , p is the probability for an infected site to stay infected while the probability of a healthy one to become infected is proportional to q and to the number of infected nearest neighbors. Similarly to the above analysis of the DP model we consider here the $2d$ contact process on a chain with discrete time steps and parallel update using occupation numbers $n_{i,t}$. For a change we assume now that $n_{i,t} = 1$ corresponds to an infected site. The CP model's transfer probabilities are

$$P(1|0,0,1) = P(1|1,0,0) = q/2, \quad P(1|1,0,1) = q, \quad P(1|*,1,*) = p, \quad P(1|0,0,0) = 0; \quad (7)$$

$$P(0|a,b,c) = 1 - P(1|a,b,c).$$

The process undergoes absorbing-active phase transition of DP class [6, 7] at

$$p_{CP}(q) \approx 1 - aq - bq^3, \quad a = 0.3, \quad b = 0.17, \quad (8)$$

with the order parameter $\rho(\infty) = 0$ at $p < p_{CP}(q)$ and $\rho(\infty) \neq 0$ at $p > p_{CP}(q)$. Here

$\rho(t) = \left\langle \sum_i n_{i,t} \right\rangle / N$. The critical line (8) shown in Fig. 4 is our fit of the MC simulation data. The CP patterns on the square time-space lattice represent $2d$ percolative clusters in the temporal direction since all infected (survived) sites have at least one ancestor at the preceding time step.

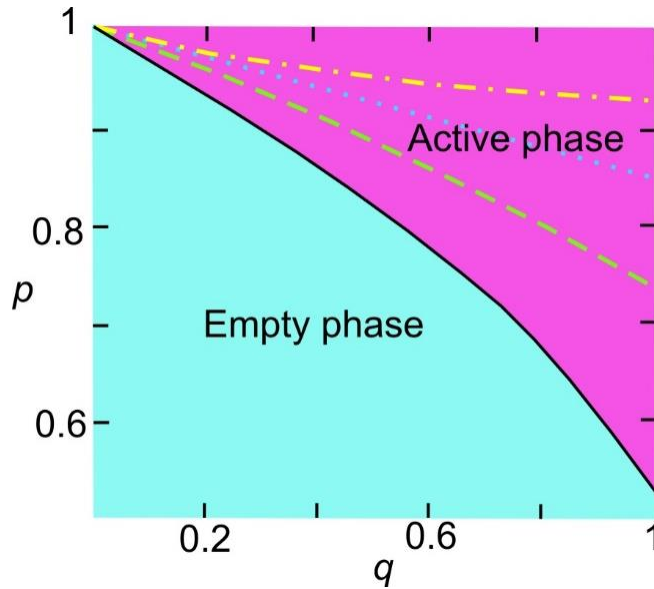


Fig. 4. *Phase diagram of contact process.* The bold black curve (8) is the boundary of the absorbing-active phase transition. The boundaries for appearance of backbones with $h = 0$ also shown. The sublattice backbone exists above dashed line, 2-site hub backbone – above dotted line and 4-site hub backbone with $f = 4$ – above dashed-dotted line.

We perform MC simulations to reveal various backbones in the percolative patterns. We consider sublattices with $(2i, 2t)$ sites, 2-site cells of $(2i, t)$, $(2i+1, t)$ sites and 4-site cells of $(2i, 2t)$, $(2i+1, 2t)$, $(2i, 2t+1)$, $(2i+1, 2t+1)$ sites. Similarly to the previously analyzed BDP model, the corresponding backbones also appear as a result of continuous geometric phase transitions. The critical lines for some of those transitions on the p - q plane are shown in Fig. 4. The critical values of parameter p at the ends of these lines ($q = 1$) are listed in Table II.

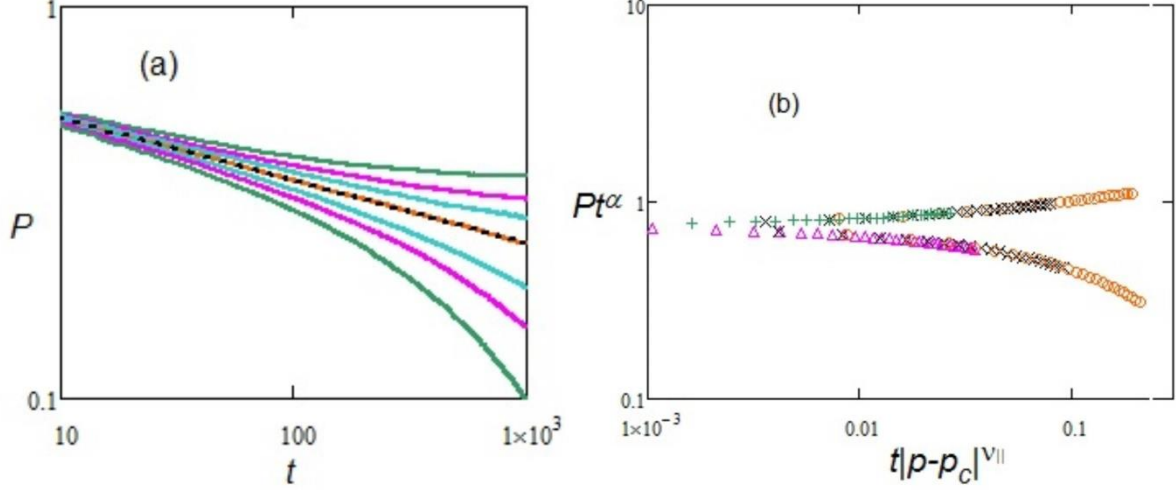


Fig. 5. (a) MC simulations of relaxation of the CP sublattice percolation capacity $P(t)$ with $h = 0$ for $q = 1$ and series of p near $p_c \approx 0.73$; from top to bottom: $p = 0.735, 0.732, 0.73, 0.7277, 0.725, 0.723, 0.72$. Dashed line corresponds to power law $0.75/t^\alpha$, with $\alpha = 0.16$. (b) Collapse of the curves from (a) onto a single scaling function. Fitting gives the values of $\nu_{||} \approx 1.735$ and $p_c = 0.7277$. The chain studied has 20000 sites with cyclic boundary conditions and raw data are averaged over 200 trials. Initial state is fully occupied one.

The CP distribution function and analytical expressions for the order parameters of various backbones can be obtained similarly to those of the BDP, cf. equations (2)-(5). Direct MC simulations of the temporal relaxation of backbone capacities demonstrate the validity of scaling at all geometrical phase transitions. The values of the critical indices $\alpha = 0.16$ and $\nu_{||} \approx 1.735$ imply that the transitions are of the DP universality class, see Fig. 5.

Table II. The transition points of contact process at $q = 1$ for several backbones.

Sublattice		2-site hubs, $f = 2$		4-site hubs		
h	$p_c(q=1)$	h	$p_c(q=1)$	f	h	$p_c(q=1)$
1	0.603(5)	1	0.732(7)	2	1	0.528(3) = p_{CP}
0	0.727(7)	0	0.840(3)	2	0	0.581(3)
				3	1	0.636(5)
				3	0	0.722(3)
				4	1	0.856(4)
				4	0	0.916(5)

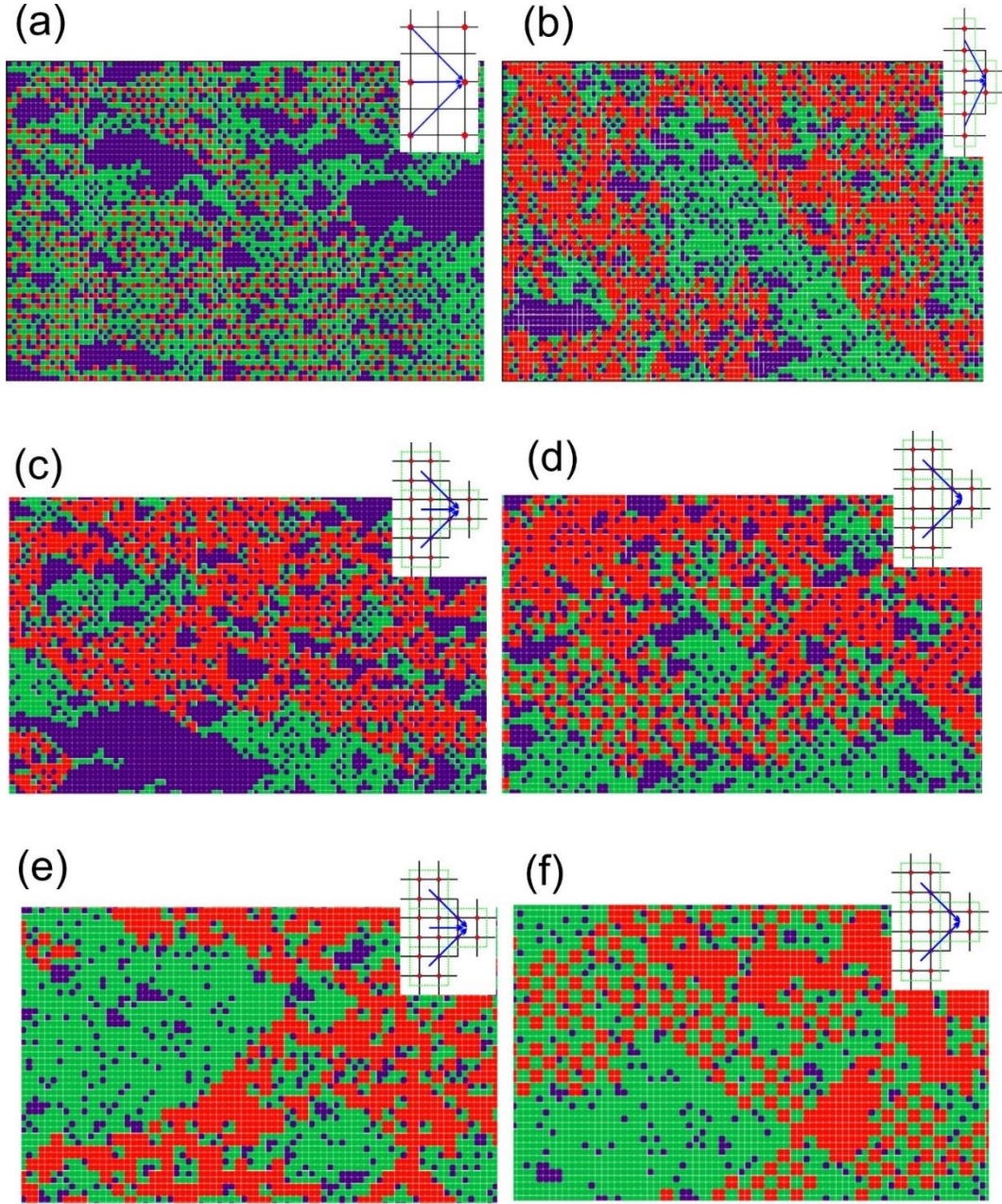


Fig. 6. *Percolative patterns of contact process*. The fragments of steady patterns of contact process at $q = 1$ (green squares) with backbones (red squares). (a) $p = 0.61$, $2a$ sublattice backbone, (b) $p = 0.74$, 2-site cells' backbone with nearest and next-nearest bonds, $f = 2$, (c) $p = 0.64$, 4-site cells' backbone with nearest and next-nearest bonds, $f = 3$, (d) $p = 0.76$, 4-site cells' backbone with next-nearest bonds, $f = 3$, (e) $p = 0.86$, 4-site cells' backbone with nearest and next-nearest bonds, $f = 4$, (f) $p = 0.92$, 4-site cells' backbone with next-nearest bonds, $f = 4$.

The percolative patterns of CP with different backbones are shown in Fig. 6. Similarly to our previous conjecture about the BDP model, we infer that the various backbones we explicitly found and analyzed for the contact process are in fact only a small set of the infinite cascade of geometric phase transitions associated with the emergence of more and more new percolative backbones.

4. Replication process

A variant of the kinetic replication process was introduced in [8]. Its transfer probabilities depend on the two parameters p and q . In the limiting cases $p \rightarrow 0$ and $p \rightarrow 1$ this process becomes BDP or CP, respectively. It was shown in [8] that besides standard absorbing-active transition there is another phase transition between two active phases. The unusual second active phase possesses a subtle percolative order. The backbone of that percolation pattern is made out of the active-dead nearest-neighbor spatial pairs unified in a connected network. Due to the analogy of that short-range spatial order to antiferromagnetic dipoles, we called it the antiferromagnetic percolative phase. In view of the relation of the model to the BDP and CP models, it is no surprise that other geometrical transitions considered above are also present in this case. In particular, our MC simulations revealed geometrical phase transitions inside the conventional active phase of the model associated with appearance of percolation via sublattices and/or coarse-grained lattices made out of various hubs. We will not give the technical details on these phases of the replication model, since they hardly give us more conceptual insights with respect to what has been presented so far. The key point is that the active phase of the model is not plain, and it also contains a cascade of geometric transitions due to the emergence of various percolative backbones.

5. Generalizations

We should note that many more percolative backbones could be considered in addition to those we have analyzed above. For instance, one can change the sum $\sum n_{i,t}$ in equation (6) into a linear combination of $n_{i,t}$. This will define some intrinsic order in the hubs, like e.g. the antiferromagnetic order in the 2-site hubs [8]. Generally, one can choose an arbitrary polynomial of the occupation numbers of the sites belonging to the hub as the argument of the Heaviside function in (6), thus defining arbitrary patterns inside the hubs.

We suggest that the multiple transitions we report here are ubiquitous and can be found in other percolation models [9-11]. Thus, one can easily show the existence of cascades of transitions in the ordinary site percolation problem. Let us take, for example, a square lattice with the probability p of each site to be filled, and coarse-grain it by introducing square hubs with s nodes

and the hub fillings $\nu_{s,f} = \mathcal{G}\left(\sum_{i \in \text{hub}} n_i - f\right)$. The probability of $\nu_{s,f} = 1$ can be readily calculated as

$$P(\nu_{s,f} = 1) = \sum_{k=f}^s \binom{s}{k} p^k (1-p)^{s-k}$$

Thus we obtain the coarse-grained square lattice built on the hubs with the new probability of a site to be filled $P(\nu_{s,f} = 1)$. For the critical points of the hub percolation $p_{s,f}$ we get the equation

$$\sum_{k=f}^s \binom{s}{k} p^k (1-p)^{s-k} = p_c$$

where $p_c = 0.593$ is the percolation threshold for a square lattice. In particular, we obtain $p_{s,s} = p_c^{1/s}$ and $p_{s,1} = 1 - (1 - p_c)^{1/s}$. Note that $p_{s,s} > p_c$ while $p_{s,1} < p_c$, the latter case we can interpret as appearance of precursor percolation.

In similar manner, one can show the appearance of inner structures in many others percolation models [9-11]. Therefore, the transitions in which various percolative backbones emerge can be seen as a generic feature of percolation.

6. Discussion and conclusion

The main result we report in this paper is the (presumably) infinite cascades of geometric phase transitions inside the percolative phases of three kinetic models. Note that a cascade of multiple transitions is something, which we know can happen in several systems. Multiple continuous and discontinuous percolation phase transitions were reported recently in several complex network models [2, 12-16]. The paradigmatic quantum Hall effect provides a well-known example of a cascade of quantum phase transitions [17, 18]. The devil's staircase of the thermal commensurate-incommensurate transitions occurs in the 3D ANNNI model [19] or in its more complicated version with the competitive in-plane interactions [20]. The experimental observations of such staircase are reported for the latter case [21].

The majority of the known multiple transitions have local variables (or their Fourier transforms) as the order parameters (OP), which are easily identified. The percolation transitions we studied belong to the other class having essentially nonlocal OPs. The singularities born by such transitions have no effect on all (or almost all) local variables. This explains why we found cascades of new transitions in the models, which have been studied for at least few decades. The previous studies were mainly concentrated on the local OP for absorbing-active transition, i.e. the average site's filling and its correlators [6, 7]. However, the study of such nonlocal variable as the survival probability in the DP model [22] revealed the signatures of multiple transitions. Numerical data of the distribution of its complex zeros show that they form a multitude of curves the ends of which tend to the real axis p with the growth of a sample. This indicates the appearance of real singularities in the thermodynamic limit. The results presented in [22] are insufficient to decide to which points these curves tend exactly. However, it is quite possible that some of these limiting points are the critical points of the geometrical transitions considered here.

The situation when the system with local transition has also nonlocal ones is not new. The notorious example is the geometric site-percolation transition of like-sign spins in the configuration patterns of Ising model [23, 24] which have no effect on the local thermodynamic variables. Similar situation exists in the Coniglio-Klein model [25] with Fortuin-Kastelein random bonds [26] on the Ising like-sign configuration patterns. The model is designed to have bond-percolation transition with the Ising singularities at $h=0$ [25, 24] but, in addition, it has percolation transition along the so-called Kertesz line in h - T plane [27, 24]. The latter has no manifestation in the thermodynamic properties of Ising model, which has analytical free energy in finite fields [28]. However, the Kertesz line manifests itself in global properties of the Ising model. According to results [29, 30] the series

expansions of the partition function of the Ising model demonstrate different convergence radii on two sides of the Kertesz line.

The simple illustration of the percolation transitions in Ising spin models, which are completely decoupled from the local variables, gives the system of independent spins in a field. Placed on some lattice with a specific set of bonds between sites, this system exhibits the site-percolation transition for the clusters of, say, + spins, while its thermodynamic (i.e. local) properties are, apparently, analytic in all h - T plane. Indeed, introducing the occupation numbers $n_r = (1 + S_r)/2$ the featureless Gibbs distribution function of the spins can be written as the site percolation distribution function:

$$\frac{e^{\beta H \sum_r S_r}}{(2 \cosh \beta H)^N} = p_+^{\sum_r n_r} (1 - p_+)^{N - \sum_r n_r}, \quad p_+ \equiv \frac{e^{\beta H}}{2 \cosh \beta H}$$

The distribution function on the r.h.s. of the above equation is the probability of a configuration where each site is filled independently with the probability p_+ . It predicts divergent connected cluster of + spins (percolation) at $p_+ > p_c$, where the critical value p_c is determined by the type of the lattice considered [9].

Some recent studies show that the simple spin models with analytical thermodynamics can exhibit other types of “hidden” nonlocal transitions beside the percolation. For example, the antiferromagnetic Ising chain in a field undergoes the transition between phases with different asymptotes of correlators of string operator [31].

These examples show that local properties of the model encoded in the partition function may not feel the presence of nonlocal transition. However, in case of nontrivial distribution function, whether the nonlocal percolation transition decouples completely from the local variables is a subtle question. In more complex systems with interaction the percolative geometric transitions can manifest themselves via crossovers of some local observables. For example, at small h the Kertesz line coincides with the line where the maximum of Ising magnetic susceptibility occurs [25]. Another example of such crossover was found in [8] in the growth of the average length of the “antiferromagnetic” clusters near the critical line where the hidden nonlocal order parameter, similar to the one given by equation (2) appears. Note that in the context of quantum condensed matter physics there were recent studies relating crossovers to specific critical points where nonlocal OPs (quantized topological phases and/or topological numbers) change. This was reported for the BEC-BCS crossover [32] and for several models of quantum chains and ladders [33-35]. Hence, it is natural to suggest that some crossovers in behavior of local variables are the indication of nonlocal transitions.

Quantum phase transitions with nonlocal (hidden) topological orders can be characterized in terms of string OPs introduced first by den Nijs and Rommelse [36]. Such order parameters are found in many low-dimensional and/or frustrated systems, topological insulators/superconductors

exhibiting various exotic quantum liquid states and transitions between them [17, 18]. In view of certain similarity of quantum string OPs with those of DP (2) we expect that cascades of topological transitions can be also found in many quantum systems using approaches similar to those we have employed.

In some cases it is possible to translate the hidden order into the local Landau framework, like, e.g. for the Kitaev model via transformations from spins to Majorana fermions and then to new dual spins which can manifest conventional long-ranged order [37]. However, there is no general recipe how to do it. The present results shows that the local Landau paradigm is implicitly preserved, since the scaling form of singularities (of DP universality class) implies strongly the existence of mappings of nonlocal theory exemplified by equations (1)-(3) onto local Landau-Ginzburg actions near corresponding transition points. However, now it is not clear how these mappings can be actually realized. This is an important direction for future work.

Acknowledgments

We thank M. Herman for careful reading of the manuscript and helpful comments. We acknowledge support from the Laurentian University Research Fund (LURF) (G.Y.C.) and from the Southern Federal University grant # 213.01-2014/011-BF (P.N.T.). The Shared Hierarchical Academic Research Computing Network (SHARCNET) and Compute/Calcul Canada generously provided facilities for carrying out numerical calculations.

REFERENCES

- [1] Boccaletti S, Latora V, Moreno Y, Chavez M and Hwang D-U. Complex networks: Structure and dynamics. Phys. Rept. 2006 **424**, 175-308.
- [2] Newman M E J. *Networks: An Introduction*. 2010 (Oxford University Press, Oxford).
- [3] Havlin S, Stanley H E, Bashan A, Gao J and Kenett D Y. Percolation of interdependent network of networks. 2015 Chaos, Soliton & Fractals **72**, 4-19.
- [4] Gao J, Buldyrev S V, Stanley H E and Havlin S. Networks formed from interdependent networks. 2012 Nature Phys. **8**, 40-48.
- [5] Gao J, Buldyrev S V, Havlin S and Stanley H E. Robustness of a network formed by n interdependent networks with a one-to-one correspondence of dependent nodes. 2012 Phys. Rev. E **85**, 066134.
- [6] Hinrichsen H. Non-equilibrium phase transitions. 2006 Physica A **369**, 1-28.
- [7] Hinrichsen, H. Non-equilibrium critical phenomena and phase transitions into absorbing states. Adv. Phys. 49, 815-958 (2000).
- [8] Timonin P N and Chitov G Y. Hidden percolation transition in kinetic replication process. 2015 J. Phys. A: Math. Theor. 48, 135003.
- [9] Stauffer D and Aharony A. *Introduction to percolation theory*, 2003 2nd revised edition (Taylor & Francis, London).
- [10] Araujo N A M, Grassberger P, Kahng B, Schrenk K J and Ziff R M. Recent advances and open challenges in percolation, 2014 Eur. Phys. J. Special Topics **223**, 2307.
- [11] Saberi A A, Recent advances in percolation theory and its applications. 2015 Physics Reports **578**, 1-32.
- [12] Colomer-de-Simon P and Boguna M. Double percolation phase transition in clustered complex networks. 2014 Phys. Rev. X 4, 041020.
- [13] Bianconi G and Dorogovtsev S N. Multiple percolation transitions in a configuration model of a network of networks. 2014 Phys. Rev. E **89**, 062814.
- [14] Chen W, Cheng X, Zheng Z, Chung N N, D'Souza R M and Nagler J. Unstable supercritical discontinuous percolation transitions. 2013 Phys. Rev. E 88, 042152.
- [15] Chen W, Nagler J, Cheng X, Jin X, Shen H, Zheng Z and D'Souza R M. Phase transitions in supercritical explosive percolation. 2013 Phys. Rev. E **87**, 052130.
- [16] Nagler J, Tiessen T and Gutch H W. Continuous percolation with discontinuities. 2012 Phys. Rev. X **2**, 031009.
- [17] Wen X-G. *Quantum Field Theory of Many-Body Systems*. 2004 (Oxford University Press, New York).
- [18] Fradkin E. *Field Theories of Condensed Matter Physics*, 2013 2nd edition (Cambridge University Press, New York).
- [19] Selke W. The ANNNI model – theoretical analysis and experimental applications. 1988 Phys. Rep. **170**, 213-264.
- [20] Chitov G Y and Gros C. On the stacking charge order in NaV_2O_5 . 2004 J. Phys.: Condens. Matter **16**, L415-L420.

- [21] Ohwada K et al. Devils staircase-type phase transition in NaV_2O_5 under high pressure. 2001 Phys. Rev. Lett. **87**, 086402.
- [22] Dammer S M, Dahmen S R and Hinrichsen H. Yang-Lee zeros for a nonequilibrium phase transition. 2002 J. Phys. A: Math. Gen. **35**, 4527-4539.
- [23] Coniglio A, Nappi C R, Peruggi F and Russo L. Percolation points and critical points of the Ising model. 1977 J. Phys. A: Math. Gen. **10**, 205-218.
- [24] Delfino G. Field theory of Ising percolating clusters. 2009 Nucl. Phys. B **818**, 196-211.
- [25] Coniglio A and Klein W. Clusters and Ising critical droplets: a renormalization group approach. 1980 J. Phys. A: Math. Gen. **13**, 2775-2780.
- [26] Fortuin C M and Kasteleyn P W. On the random-cluster model. I. Introduction and relation to other models. 1972 Physica **57**, 536-564.
- [27] Kertész J. Existence of weak singularities when going around the liquid-gas critical point. 1989 Physica A **161**, 58-62.
- [28] Lee T D and Yang C N. Statistical theory of equations of state and phase transitions. II. Lattice gas and Ising model. 1952 Phys. Rev. **87**, 410-419.
- [29] Adler J and Stauffer D. Search for liquid-gas transition above the critical temperature. 1991 Physica A **175**, 222-228.
- [30] Janke W, Johnston D A and Stathakopoulos M. A Kertesz line on planar random graphs. 2002 J. Phys. A: Math. Gen. **35**, 7575-7584.
- [31] Ivanov D A and Abanov A G. Characterizing correlations with full counting statistics: Classical Ising and quantum XY spin chains. 2013 Phys. Rev. E **87**, 022114.
- [32] Arikawa M, Maruyama I and Hatsugai Y. Topological quantum phase transition in the BEC-BCS crossover. 2010 Phys. Rev. B **82**, 073105.
- [33] Maruyama I, Hirano T and Hatsugai Y. Topological identification of a spin-1/2 two-leg ladder with four-spin ring exchange. 2009 Phys. Rev. B **79**, 115107.
- [34] Chepiga N, Michaud F and Mila F. Berry phase investigation of spin-S ladders. 2013 Phys. Rev. B **88**, 184418.
- [35] Ezawa M, Tanaka Y and Nagaosa N. Topological phase transition without gap closing. 2013 Sci. Rep. **3**, 2790, 1-9.
- [36] den Nijs M and Rommelse K. Preroughening transitions in crystal surfaces and valence-bond phases in quantum spin chains. 1989 Phys. Rev. B **40**, 4709-4734.
- [37] Feng X-Y, Zhang G-M and Xiang T. Topological characterization of quantum phase transitions in a spin-1/2 model. 2007 Phys. Rev. Lett. **98**, 087204.